Hartree-Fock treatment of the two-component Bose-Einstein condensate

Patrik Öhberg and Stig Stenholm
Helsinki Institute of Physics, University of Helsinki, P.O. Box 9, FIN-00014, Helsinki, Finland
and Department of Physics, Royal Institute of Technology, Lindstedtsvägen 24, S-10044 Stockholm, Sweden
(Received 14 August 1997)

We present a numerical study of a trapped binary Bose-condensed gas by solving the corresponding Hartree-Fock equations. The density profile of the binary Bose gas is solved with a harmonic trapping potential as a function of temperature in two and three dimensions. We find a symmetry breaking in the two-dimensional case where the two condensates separate. We also present a phase diagram in the three-dimensional case of the different regions where the binary condensate becomes a single condensate and eventually an ordinary gas as a function of temperature and the interaction strength between the atoms. [S1050-2947(98)06502-0]

PACS number(s): 03.75.Fi, 05.30.Jp

I. INTRODUCTION

The recent realization of Bose-Einstein condensation in dilute gases of trapped alkali-metal atoms has provided an opportunity to investigate macroscopic quantum effects in recently developed systems [1–3]. The second generation of experiments on condensates in Rb and Na vapors [4–8] give detailed information about the condensate long-range order, which distinguishes them from an ordinary gas. These atoms are known to have a positive scattering length, i.e., the atoms experience a repulsive force between them. Recent experiments with Li [9] show that for a limited range of particle densities even particles with negative scattering length can form a condensate. In a recent experiment Myatt *et al.* have been able to trap atoms of two different spin states and cool them below the condensate transition point [8]. These experiments give us knowledge about the condensation in a whole different dynamical regime.

Much work on the density distribution of the condensate has been carried out for a single condensate and lately also for the two-component condensate [10–12]. These calculations have been valid mainly at the temperatures $T=0$. In our earlier paper we solved the Hartree-Fock equations for a single condensate [13]. In this paper we derive and solve numerically the Hartree-Fock equations for a two-component gas trapped in harmonic external potentials at a finite temperature. We solve for the density in two and three dimensions for the case with simple harmonic potentials. The Hartree-Fock (HF) equations give a phase transition at the onset of condensation, but they do not take into account any critical fluctuations. It is possible, however, to obtain a qualitative picture of the features of the Bose-Einstein phase transition using the HF approach.

In a real experiment, the different potentials experienced by the two components make them respond differently to gravity. This separates the condensed clouds in space, but we assume this effect to be compensated by technical means. In this way we can investigate the intrinsic effects determined by the physically more essential interactions. The two components of the condensate repell each other, and if they form exactly on top of each other, the more weakly trapped one is pushed to expand away from the center. This is found to lead to a condensate component that has a minimum at its center. This situation is still not optimal because energy can be lowered by separating the condensates. In a symmetric trap this implies a breaking of the symmetry; the two peaks are shifted in a direction not fixed by the external potentials. We investigate this symmetry breaking in a two-dimensional model trap because solving for the asymmetric condensate proves to be numerically demanding. The calculations are found to verify the intuitive picture described.

If the two components did not interact, the condensates would form and disappear independently, thus showing two different transition temperatures. With condensate interactions, the presence of one condensate will affect the formation of the other one. This will shift the transition temperatures depending on the strength of the interaction between the two components. In particular, we expect a repulsive interaction to work against the simultaneous formation of both condensates. Thus we expect to see a modification of the phase diagram in the plane of temperature and interaction between the components. In order to keep the numerical effort manageable, we investigate this effect in a spherically symmetric three-dimensional trap. We find that the interaction shifts the boundary between the two- and one-condensate regions. We even find a case where there is no formation of a single-condensate region.

The organization of the paper is as follows. Section II reviews the HF equations that we solve numerically. In Sec. III we briefly go through the numerical methods that have been used. The results of the calculations are presented in Sec. IV, where various situations are compared. Finally, Sec. V comments on the calculations and their results.

II. HARTREE-FOCK EQUATIONS FOR THE TWO-COMPONENT CONDENSATE

The Hamiltonian for an interacting Bose gas of two different kinds of atoms can be written in the form

$$\hat{H}=\hat{H}_1+\hat{H}_2+\hat{H}_3, \tag{1}$$

where

$$\hat{H}_1=\int d\mathbf{r}\ \psi_1^\dagger(\mathbf{r})\left[-\frac{\hbar^2}{2m_1}\nabla^2+U_1(\mathbf{r})\right]\psi_1(\mathbf{r})+\frac{1}{2}\int d\mathbf{r}\int d\mathbf{r}'\psi_1^\dagger(\mathbf{r}')\psi_1^\dagger(\mathbf{r})V_1(\mathbf{r}-\mathbf{r}')\psi_1(\mathbf{r})\psi_1(\mathbf{r}'),$$

$$\hat{H}_2=\int d\mathbf{r}\ \psi_2^\dagger(\mathbf{r})\left[-\frac{\hbar^2}{2m_2}\nabla^2+U_2(\mathbf{r})\right]\psi_2(\mathbf{r})+\frac{1}{2}\int d\mathbf{r}\int d\mathbf{r}'\psi_2^\dagger(\mathbf{r}')\psi_2^\dagger(\mathbf{r})V_2(\mathbf{r}-\mathbf{r}')\psi_2(\mathbf{r})\psi_2(\mathbf{r}'), \tag{2}$$

$$\hat{H}_3=\frac{1}{2}\int d\mathbf{r}\int d\mathbf{r}'\psi_1^\dagger(\mathbf{r}')\psi_2^\dagger(\mathbf{r})V_{int}(\mathbf{r}-\mathbf{r}')\psi_1(\mathbf{r})\psi_2(\mathbf{r}'),$$

and $\psi_1,\psi_1^\dagger,\psi_2$, and $\psi_2^\dagger$ are the Boson field operators that obey the commutation rule

$$[\psi_i(\mathbf{r}),\psi_j^\dagger(\mathbf{r}')]=\delta_{ij}\delta(\mathbf{r}-\mathbf{r}'). \tag{3}$$

$U_1(\mathbf{r})$ and $U_2(\mathbf{r})$ are the two different external traps that confine the atoms. We are here going to use the short-range approximation for the interaction both between the particles of the same kind and between the two different kinds of particles. This gives us the interaction potentials ($i=1,2$)

$$V_i(\mathbf{r}-\mathbf{r}')=v_i\delta(\mathbf{r}-\mathbf{r}'), \tag{4}$$

$$V_{int}(\mathbf{r}-\mathbf{r}')=w\,\delta(\mathbf{r}-\mathbf{r}'), \tag{5}$$

where

$$v_i=\frac{4\pi\hbar^2 a_i}{m_i},\quad w=\frac{4\pi\hbar^2 a_{12}}{\sqrt{m_1m_2}}, \tag{6}$$

with the s-wave scattering lengths a_1,a_2, and a_{12}. Our goal is to calculate the temperature dependence of the two gases. We therefore introduce the thermodynamic free energy $\Omega(T,\mu)$, which is defined as

$$e^{-\beta\Omega}=\mathrm{Tr}[e^{-\beta(\hat{H}-\mu_i\hat{N}^{(i)})}], \tag{7}$$

where $\{\mu_1,\mu_2\}$ are the chemical potentials and $\mu_i\hat{N}^{(i)}$ is a sum over the two different gases. We then use a thermodynamic variational principle

$$\Omega(\hat{H})\leqslant\Omega(\hat{H}^t)+\langle(\hat{H}-\hat{H}^t)\rangle_t, \tag{8}$$

where

$$\langle\hat{A}\rangle_t\equiv\frac{\mathrm{Tr}[e^{\beta(\hat{H}^t-\mu_i\hat{N}^{(i)})}\hat{A}]}{\mathrm{Tr}[e^{\beta(\hat{H}^t-\mu_i\hat{N}^{(i)})}]} \tag{9}$$

and $\hat{H}^t$ is a single-particle trial Hamiltonian

$$\hat{H}^t=\hat{H}_1^t+\hat{H}_2^t=\sum_\alpha\{E_\alpha^{(1)}a_\alpha^\dagger a_\alpha+E_\alpha^{(2)}b_\alpha^\dagger b_\alpha\}=\sum_\alpha\int d\mathbf{r}\{E_\alpha^{(1)}|\varphi_\alpha(\mathbf{r})|^2a_\alpha^\dagger a_\alpha+E_\alpha^{(2)}|\phi_\alpha(\mathbf{r})|^2b_\alpha^\dagger b_\alpha\}. \tag{10}$$

This gives for the thermodynamic potential

$$\Omega(\hat{H})\leqslant\Omega(\hat{H}_1^t)+\Omega(\hat{H}_2^t)+\langle\hat{H}_1-\hat{H}_1^t\rangle_t+\langle\hat{H}_2-\hat{H}_2^t\rangle_t+\langle\hat{H}_3\rangle_t. \tag{11}$$

The single-particle states φ_α and ϕ_α are to be determined such that they minimize the thermodynamic free energy Ω. We now expand our field operators

$$\psi_1(\mathbf{r})=\sum_\alpha\varphi_\alpha(\mathbf{r})a_\alpha, \tag{12}$$

$$\psi_2(\mathbf{r})=\sum_\alpha\phi_\alpha(\mathbf{r})b_\alpha. \tag{13}$$

Inserting this expansion into Eq. (1) gives the Hamiltonians

$$\hat{H}_1=\int d\mathbf{r}\sum_\alpha\varphi_\alpha^*(\mathbf{r})\left[-\frac{\hbar^2}{2m_1}\nabla^2+U_1(\mathbf{r})\right]\varphi_\alpha(\mathbf{r})a_\alpha^\dagger a_\alpha+\frac{1}{2}v_1\int d\mathbf{r}\sum_{\alpha,\beta,\gamma,\delta}\varphi_\alpha^*(\mathbf{r})\varphi_\beta^*(\mathbf{r})\varphi_\gamma(\mathbf{r})\varphi_\delta(\mathbf{r})a_\alpha^\dagger a_\beta^\dagger a_\gamma a_\delta, \tag{14}$$

$$\hat{H}_2=\int d\mathbf{r}\sum_\alpha\phi_\alpha^*(\mathbf{r})\left[-\frac{\hbar^2}{2m_2}\nabla^2+U_2(\mathbf{r})\right]\phi_\alpha(\mathbf{r})b_\alpha^\dagger b_\alpha+\frac{1}{2}v_2\int d\mathbf{r}\sum_{\alpha,\beta,\gamma,\delta}\phi_\alpha^*(\mathbf{r})\phi_\beta^*(\mathbf{r})\phi_\gamma(\mathbf{r})\phi_\delta(\mathbf{r})b_\alpha^\dagger b_\beta^\dagger b_\gamma b_\delta, \tag{15}$$

$$\hat{H}_3=w\int d\mathbf{r}\sum_{\alpha,\beta,\gamma,\delta}\varphi_\alpha^*(\mathbf{r})\phi_\beta^*(\mathbf{r})\phi_\gamma(\mathbf{r})\varphi_\delta(\mathbf{r})a_\alpha^\dagger b_\beta^\dagger b_\gamma a_\delta. \tag{16}$$

We can now use the single-particle Hamiltonians and rewrite the thermodynamic free energy as

$$\Omega=\Omega_1^t+\Omega_2^t+\int d\mathbf{r}\ \widetilde{\Omega}(\mathbf{r}), \tag{17}$$

where ($i=1,2$)

$$\Omega_i^t=-\frac{1}{\beta}\sum_\alpha\ln[1-e^{-\beta(E_\alpha^{(i)}-\mu_i)}] \tag{18}$$

and $\widetilde{\Omega}=\widetilde{\Omega}_1+\widetilde{\Omega}_2+\widetilde{\Omega}_3$ with

$$\widetilde{\Omega}_1(\mathbf{r})=\sum_\alpha \varphi_\alpha^*(\mathbf{r})\left[-\frac{\hbar^2}{2m_1}\nabla^2+U_1(\mathbf{r})-E_\alpha^{(1)}\right]\varphi_\alpha(\mathbf{r})\langle N_\alpha^{(1)}\rangle_t + \frac{v_1}{2}\sum_\alpha |\varphi_\alpha(\mathbf{r})|^4\langle N_\alpha^{(1)}(N_\alpha^{(1)}-1)\rangle_t + v_1\sum_{\alpha\neq\beta}|\varphi_\alpha(\mathbf{r})|^2|\varphi_\beta(\mathbf{r})|^2\langle N_\alpha^{(1)}N_\beta^{(1)}\rangle_t, \quad (19)$$

$$\widetilde{\Omega}_2(\mathbf{r})=\sum_\alpha \phi_\alpha^*(\mathbf{r})\left[-\frac{\hbar^2}{2m_2}\nabla^2+U_2(\mathbf{r})-E_\alpha^{(2)}\right]\phi_\alpha(\mathbf{r})\langle N_\alpha^{(2)}\rangle_t + \frac{v_2}{2}\sum_\alpha |\phi_\alpha(\mathbf{r})|^4\langle N_\alpha^{(2)}(N_\alpha^{(2)}-1)\rangle_t + v_2\sum_{\alpha\neq\beta}|\phi_\alpha(\mathbf{r})|^2|\phi_\beta(\mathbf{r})|^2\langle N_\alpha^{(2)}N_\beta^{(2)}\rangle_t, \quad (20)$$

$$\widetilde{\Omega}_3(\mathbf{r})=w\sum_{\alpha,\beta}|\varphi_\alpha(\mathbf{r})|^2|\phi_\beta(\mathbf{r})|^2\langle N_\alpha^{(1)}N_\beta^{(2)}\rangle_t. \quad (21)$$

Here we have used the independent-particle properties of $\hat{H}_1^t$ and $\hat{H}_2^t$ with $N_\alpha^{(1)}=a_\alpha^\dagger a_\alpha$, $N_\alpha^{(2)}=b_\alpha^\dagger b_\alpha$, and $\langle a_\alpha^\dagger a_\alpha b_\beta^\dagger b_\beta\rangle_t = \langle N_\alpha^{(1)}\rangle_t\langle N_\beta^{(2)}\rangle_t$. In order to calculate the single-particle states φ_α and ϕ_α that minimizes the free energy Ω we have to calculate the functional derivatives

$$\frac{\delta}{\delta\varphi_\alpha^*(\mathbf{r})}\int d\mathbf{r}\ \widetilde{\Omega}[\varphi_\alpha^*(\mathbf{r}),\phi_\alpha^*(\mathbf{r})]=0, \quad (22)$$

$$\frac{\delta}{\delta\phi_\alpha^*(\mathbf{r})}\int d\mathbf{r}\ \widetilde{\Omega}[\varphi_\alpha^*(\mathbf{r}),\phi_\alpha^*(\mathbf{r})]=0. \quad (23)$$

For the $\widetilde{\Omega}_1$ and $\widetilde{\Omega}_2$ parts we can use the results for the single condensate [15,14]. From Eqs. (22) and (23) we then get the equations

$$\left[-\frac{\hbar^2}{2m_1}\nabla^2+U_1(\mathbf{r})-E_\alpha^{(1)}\right]\varphi_\alpha(\mathbf{r})\langle N_\alpha^{(1)}\rangle_t + v_1\left\{|\varphi_\alpha(\mathbf{r})|^2\langle N_\alpha^{(1)}(N_\alpha^{(1)}-1)\rangle_t + \sum_\beta \langle N_\beta^{(1)}\rangle_t|\varphi_\beta(\mathbf{r})|^2\langle N_\alpha^{(1)}\rangle\right\}\varphi_\alpha(\mathbf{r}) + w\sum_\beta |\phi_\beta(\mathbf{r})|^2\langle N_\beta^{(2)}\rangle_t\langle N_\alpha^{(1)}\rangle_t\varphi_\alpha(\mathbf{r})=0, \quad (24)$$

$$\left[-\frac{\hbar^2}{2m_2}\nabla^2+U_2(\mathbf{r})-E_\alpha^{(2)}\right]\phi_\alpha(\mathbf{r})\langle N_\alpha^{(2)}\rangle_t + v_2\left\{|\phi_\alpha(\mathbf{r})|^2\langle N_\alpha^{(2)}(N_\alpha^{(2)}-1)\rangle_t + \sum_\beta \langle N_\beta^{(2)}\rangle_t|\phi_\beta(\mathbf{r})|^2\langle N_\alpha^{(2)}\rangle_t\right\}\phi_\alpha(\mathbf{r}) + w\sum_\beta |\varphi_\beta(\mathbf{r})|^2\langle N_\beta^{(1)}\rangle_t\langle N_\alpha^{(2)}\rangle_t\phi_\alpha(\mathbf{r})=0. \quad (25)$$

We also keep in mind the difference between the condensed phase and the normal phase concerning the single-particle averages (see Ref. [13])

$$\langle N_\alpha^{(i)}N_\beta^{(i)}\rangle_t=\langle N_\alpha^{(i)}\rangle_t\langle N_\beta^{(i)}\rangle_t, \quad \alpha\neq\alpha_0, i=1,2 \quad (26)$$

$$\langle N_\alpha^{(i)}(N_\alpha^{(i)}-1)\rangle_t=2\langle N_\alpha^{(i)}\rangle_t^2, \quad \alpha\neq\alpha_0, i=1,2 \quad (27)$$

$$\langle N_{\alpha_0}^{(i)}(N_{\alpha_0}^{(i)}-1)\rangle_t=N_0^{(i)}(N_0^{(i)}-1)\approx N_0^{(i)^2}. \quad (28)$$

We can now have three different regions depending on the parameters: two condensates, a condensed phase and a normal phase, or finally two normal phases. The following are the three sets of equations.

A. Two condensates

The temperature is now below the critical temperature T_1^c and T_2^c for both gases and we have

$$\left[-\frac{\hbar^2}{2m_1}\nabla^2+U_1(\mathbf{r})+v_1[2\rho_n^1(\mathbf{r})+\rho_0^1(\mathbf{r})]+w\Gamma_1(\mathbf{r})\right]\varphi_{\alpha_0}(\mathbf{r}) = E_{\alpha_0}^{(1)}\varphi_{\alpha_0}(\mathbf{r}), \quad (29)$$

$$\left[-\frac{\hbar^2}{2m_1}\nabla^2+U_1(\mathbf{r})+2v_1[\rho_n^1(\mathbf{r})+\rho_0^1(\mathbf{r})]+w\Gamma_1(\mathbf{r})\right]\varphi_\alpha(\mathbf{r}) = E_\alpha^{(1)}\varphi_\alpha(\mathbf{r}), \quad (30)$$

$$\left[-\frac{\hbar^2}{2m_2}\nabla^2+U_2(\mathbf{r})+v_2[2\rho_n^2(\mathbf{r})+\rho_0^2(\mathbf{r})]+w\Gamma_2(\mathbf{r})\right]\phi_{\alpha_0}(\mathbf{r}) = E_{\alpha_0}^{(2)}\phi_{\alpha_0}(\mathbf{r}), \quad (31)$$

$$\left[-\frac{\hbar^2}{2m_2}\nabla^2+U_2(\mathbf{r})+2v_2[\rho_n^2(\mathbf{r})+\rho_0^2(\mathbf{r})]+w\Gamma_2(\mathbf{r})\right]\phi_\alpha(\mathbf{r}) = E_\alpha^{(2)}\phi_\alpha(\mathbf{r}), \quad (32)$$

where

$$\rho_n^1(\mathbf{r})=\sum_{\alpha\neq\alpha_0}\langle N_\alpha^{(1)}\rangle_t|\varphi_\alpha(\mathbf{r})|^2, \quad (33)$$

$$\rho_0^1(\mathbf{r})=N_{\alpha_0}^{(1)}|\varphi_{\alpha_0}(\mathbf{r})|^2, \quad (34)$$

$$\rho_n^2(\mathbf{r})=\sum_{\alpha\neq\alpha_0}\langle N_\alpha^{(2)}\rangle_t|\phi_\alpha(\mathbf{r})|^2, \quad (35)$$

$$\rho_0^2(\mathbf{r})=N_{\alpha_0}^{(2)}|\phi_{\alpha_0}(\mathbf{r})|^2, \quad (36)$$

$$\Gamma_1(\mathbf{r})=N_{\alpha_0}^{(2)}|\phi_{\alpha_0}(\mathbf{r})|^2+\sum_{\alpha\neq\alpha_0}\langle N_\alpha^{(2)}\rangle_t|\phi_\alpha(\mathbf{r})|^2, \quad (37)$$

$$\Gamma_2(\mathbf{r})=N_{\alpha_0}^{(1)}|\varphi_{\alpha_0}(\mathbf{r})|^2+\sum_{\alpha\neq\alpha_0}\langle N_\alpha^{(1)}\rangle_t|\varphi_\alpha(\mathbf{r})|^2, \quad (38)$$

$$\langle N_\alpha^{(i)}\rangle_t=1/(e^{\beta(E_\alpha^{(i)}-\mu_i)}-1), \quad i=1,2. \quad (39)$$

B. A condensed phase and a normal phase

The temperature is now below one of the critical temperatures. We give here the equations with system (1) in the condensed phase. Then the system to be solved consists of Eqs. (29) and (30) and in the noncondensed phase

$$\left[-\frac{\hbar^2}{2m_2}\nabla^2+U_2(\mathbf{r})+2v_2\rho^2(\mathbf{r})+w\Gamma_2(\mathbf{r})\right]\phi_\alpha(\mathbf{r}) = E_\alpha^{(2)}\phi_\alpha(\mathbf{r}), \tag{40}$$

with $\rho^2(\mathbf{r})=\rho_0^2(\mathbf{r})+\rho_n^2(\mathbf{r})$.

C. Two normal phases

The temperature is here above the critical temperature for both gases and the equations are

$$\left[-\frac{\hbar^2}{2m_1}\nabla^2+U_1(\mathbf{r})+2v_1\rho^1(\mathbf{r})+w\Gamma_1(\mathbf{r})\right]\varphi_\alpha(\mathbf{r}) = E_\alpha^{(1)}\varphi_\alpha(\mathbf{r}), \tag{41}$$

$$\left[-\frac{\hbar^2}{2m_2}\nabla^2+U_2(\mathbf{r})+2v_2\rho^2(\mathbf{r})+w\Gamma_2(\mathbf{r})\right]\phi_\alpha(\mathbf{r}) = E_\alpha^{(2)}\phi_\alpha(\mathbf{r}), \tag{42}$$

with $\rho^i(\mathbf{r})=\rho_0^i(\mathbf{r})+\rho_n^i(\mathbf{r})$. The chemical potentials μ_1 and μ_2 are calculated from the particle numbers

$$N^{(i)}=\sum_\alpha \frac{1}{e^{\beta(E_\alpha^{(i)}-\mu_i)}-1}, \quad i=1,2. \tag{43}$$

In the condensed phase we have $\mu_1=E_{\alpha_0}^{(1)}$ and $\mu_2=E_{\alpha_0}^{(2)}$.

III. NUMERICAL METHODS

The numerical methods have been thoroughly explained in Ref. [13]. We are here only going to give the general ideas. The equations are highly nonlinear and therefore have to be solved iteratively. This means that we start by guessing the densities and solving the ordinary differential equations. The resulting eigenvalues and eigenstates are then used to obtain new densities. This procedure is then iterated until we have a self-consistent solution. In the experiments with Bose-condensed gases the trapping potential has been approximately harmonic. The two gases have different external potentials because they are trapped in different spin states. This then gives us the two different external potentials

$$U_i(x,y,z)=\frac{1}{2}m_i(\Omega_{x_i}^2x^2+\Omega_{y_i}^2y^2+\Omega_{z_i}^2z^2), \quad i=1,2. \tag{44}$$

Because of the harmonic external potentials, a natural approach would be to expand the solutions in the harmonic-oscillator eigenfunctions

$$\varphi(\mathbf{r})=\sum_i a_i\Phi_i^{HO}. \tag{45}$$

The problem then reduces to an eigenvalue problem for the expansion coefficients a_i. In the actual calculations we have at most four coupled equations that have to be solved simultaneously. This is not a problem since we have basically the same situation as in the single-condensate case. The only drawback is the computing time, which is doubled compared to the calculations in Ref. [13].

The method of expansion in harmonic-oscillator eigenfunctions is especially good in asymmetric environments. However, if we have a spherically symmetric geometry, we can easily discretize our solutions on a lattice, $\varphi(r)\rightarrow\varphi_i$, and the derivatives turn into differences, which then gives us a tridiagonal eigenvalue problem whose solutions directly gives the desired quantities. This method works best in situations where the problem is effectively one dimensional.

IV. RESULTS

In this paper we calculate the density of the two-component condensate in a harmonic trap in two and three dimensions including asymmetry in the two-dimensional case. We also present a phase diagram for a three-dimensional spherically symmetric trap. The equations are put into dimensionless form by the scaling

$$r=\frac{\hbar^{1/2}}{[m_1m_2\Omega_1\Omega_2]^{1/4}}r' \tag{46}$$

and $x=\lambda x', y=\lambda y'$ with

$$\lambda=\frac{\hbar^{1/2}}{[m_1m_2]^{1/2}[\Omega_{x_1}\Omega_{x_2}\Omega_{y_1}\Omega_{y_2}]^{1/8}}. \tag{47}$$

This gives us the dimensionless energies scaled to

$$\tfrac{1}{2}\hbar(\Omega_{x_1}\Omega_{x_1}\Omega_{y_1}\Omega_{y_2})^{1/4}\sqrt{m_2/m_1}$$

and

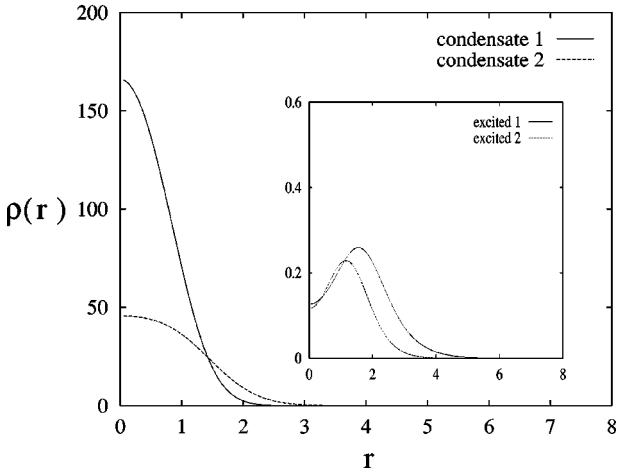

FIG. 1. Spherically symmetric density of the two condensates. The two condensates hardly ''see'' each other at $w=0.012$. The inset shows the excited part. The temperature is here $T=3.33$ and the interactions $v_1=0.02$ and $v_2=0.01$ with $N^{(1)}=1000$ and $N^{(2)}=1000$. The numbers in all figures are expressed in harmonic-oscillator units according to Eqs. (46) and (47).

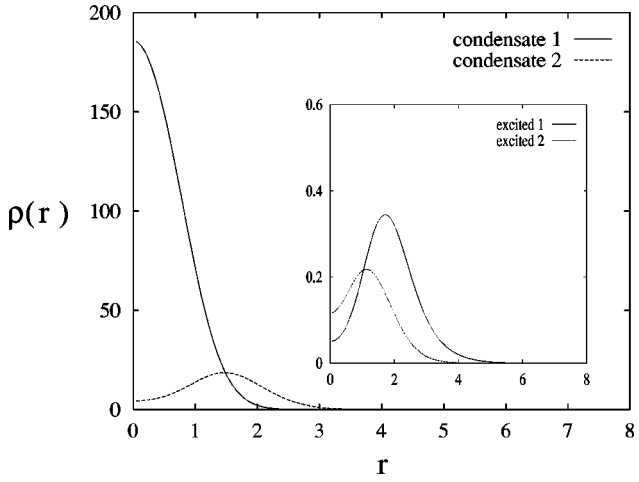

FIG. 2. Same situation as in Fig. 1, but with a stronger mutual interaction $w=0.05$. Here we can see that the $N^{(2)}$ particles are pushed away from the center.

$$\tfrac{1}{2}\hbar(\Omega_{x_1}\Omega_{x_1}\Omega_{y_1}\Omega_{y_2})^{1/4}\sqrt{m_1/m_2}.$$

A. Density calculations

The most natural thing to calculate from the Hartree-Fock equations are the densities. In the spherically symmetric case we have the external potentials

$$U_i(r)=\frac{1}{2}m_i\Omega_i^2 r^2, \quad i=1,2. \tag{48}$$

Throughout the calculations in this paper we have chosen the ratio between m_1 and m_2 to be $m_1/m_2=1$ and the interactions v_1 and v_2 to be $v_1=0.02$ and $v_2=0.01$. In our scaled units these correspond closely to the realistic values. In Fig. 1 we show the spherically symmetric density for the two condensates with $N=1000$ particles in both gases and the interaction strength between the different particles is set to $w=0.012$ with $\Omega_1/\Omega_2=2.0$. Here we can see that the two different particles hardly ''know'' anything about each other. The inverse temperature is here $\beta=0.3$. In Fig. 2 we have increased the interaction strength w to $w=0.05$. The condensate of the more weakly interacting particles is pushed away from the center of the trap and is forming a shell around the particles in the center of the trap. These results were obtained by spherically symmetric eigensolutions, which means that we can say nothing about the existence of states with lower energy that could possess an asymmetric geometry. This suggests to look for a solution of an asymmetric two-component condensate.

It is extremely time and memory consuming to solve the full three-dimensional asymmetric case. We therefore concentrate on the two-dimensional two-component condensate. We then have the external potentials

$$U_i(x,y)=\frac{1}{2}m_i(\Omega_{x_i}^2x^2+\Omega_{y_i}^2y^2), \quad i=1,2. \tag{49}$$

In the two-dimensional calculations we have chosen the asymmetry of the trap to be

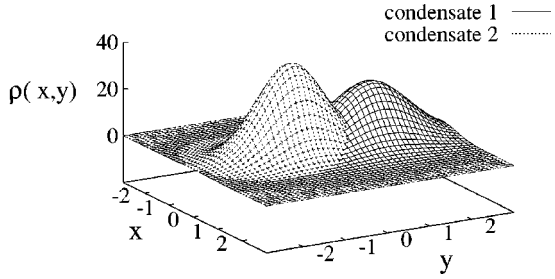

FIG. 3. Two-dimensional asymmetric case where the condensates have formed two separate peaks around the center of the trap. The interaction is here $w=0.1$ with $\Omega_x/\Omega_y=\sqrt{8}$, $\Omega_{\alpha_1}/\Omega_{\alpha_2}=1/\sqrt{2}$, and the temperature $T=1.0$. The iteration is here started away from the center with two Gaussian condensate densities at (1,1) and $(1,-1)$. The ground-state energies are $E_0^{(1)}=3.082$ and $E_0^{(2)}=3.584$.

$$\frac{\Omega_{x_i}}{\Omega_{y_i}}=\sqrt{8}, \quad i=1,2 \tag{50}$$

with $\Omega_{\alpha_1}/\Omega_{\alpha_2}=1/\sqrt{2}$ and $N^{(1)}=N^{(2)}=100$. In Figs. 3–5 we show the density of the two condensates at the inverse temperature $\beta=1.0$. If we start the iteration by setting the initial densities to, for instance, $x=1,y=1$ and $x=1,y=-1$, we end the iteration with two separated condensates aligned in the weaker trap direction. In Fig. 3 we have used $w=0.1$ and in Fig. 4 we have increased the interaction to $w=0.3$, where we can see that the two condensates get pushed further away from each other with increasing interaction strength. However, if we start by putting both condensates at the center of the trap, we get a stable solution that is symmetric also in the weaker trap direction and does not show a separation into two displaced condensates. This is shown in Fig. 5. The ground-state energy for this case is higher than in the purely asymmetric situation, which suggests that the spontaneous symmetry breaking occurs. This is more clearly seen if we look at the two-dimensional rotationally symmetric potential. Starting the iteration with the initial densities away from the center gives us two condensates separated into two distinct peaks, where the weaker trapped condensate is slightly wrapped around the other one. This is shown in Fig. 6 with $\beta=1.0$ and $w=0.2$. In Fig. 7 we have the same situation, but now we start the iteration with the densities at the center of the trap. The calculation converges nicely and the stable solution shows a condensate peak in the center and a ring formed by the weaker trapped atoms around it.

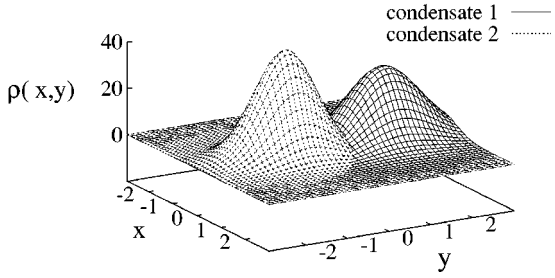

FIG. 4. Same situation as in Fig. 3, but with the stronger interaction $w=0.3$. The two condensates are pushed further away from each other because of their stronger repulsive interaction.

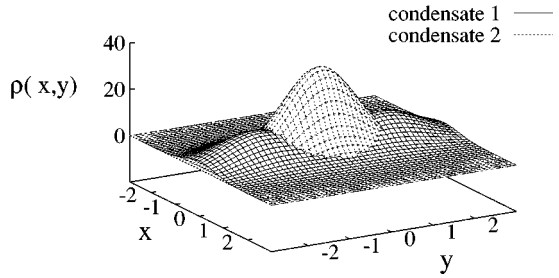

FIG. 5. Same situation as in Fig. 3. The iteration is here started with the condensates in the center of the trap with $w=0.1$ and $T=1.0$. The condensates sit on top of each other. The ground-state energy is higher than in the asymmetric formation, with $E_0^{(1)}=3.241$ and $E_0^{(2)}=3.677$; cf. the values given in Fig. 3.

B. Phase diagram

The Hartree-Fock equations do not describe exactly the transition region between an ordinary gas and a Bose-condensed one, but they do suggest a general view of what is going on. If we define the critical temperature as the temperature where the number of particles in the condensate goes to zero, we can calculate this number of particles with the equations for $T<T_c$ at different temperatures until we reach the point where all particles in the condensate have been depleted. In Fig. 8 we show three phase diagrams as a function of temperature and interaction strength w, with fixed numbers of particles $N^{(1)}=100$ and $N^{(2)}$ varying between 100 and 728. We see that three regions need to be covered. We first solve the equations for two condensates with a fixed w and increase the temperature until one of the condensates disappears, where we find our phase transition. Increasing the temperature even more means that we are in the one-condensed-phase–one-normal-phase region and we have to use Eqs. (29), (30), and (40). Increasing the temperature further finally destroys the remaining condensate and we have found our second transition point. This kind of calculation has been repeated for different interaction strengths and particle numbers. Adjusting the particle numbers so that the two transition lines almost coincide, we find that there exists a region where one can go from two condensates to normal gases by lowering the temperature. This situation is shown in Fig. 8(b). The phenomena exhibited in our phase diagrams may not give an accurate picture of the real systems, but they can be believed to suggest the trends expected in the actual experiments.

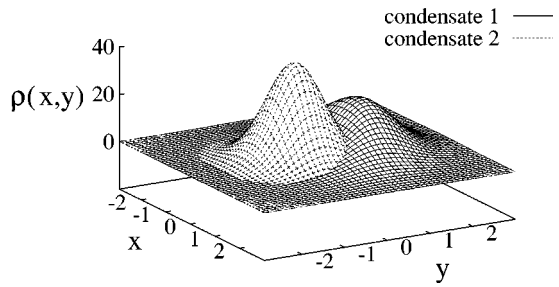

FIG. 6. Two-dimensional spherically symmetric situation with $w=0.2$, where we find two separate density peaks with the ground state energies $E_0^{(1)}=3.465$ and $E_0^{(2)}=3.596$. One can clearly see the wrap around effect by the more weakly trapped condensate. The iteration is started away from the center.

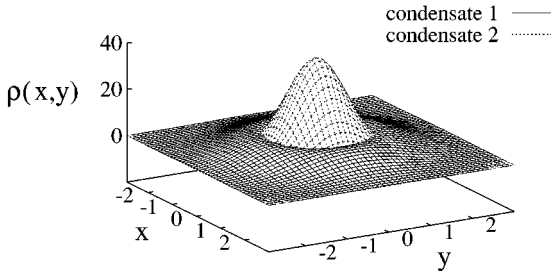

FIG. 7. Two condensates situated in the center of the trap on top of each other. The iteration is started with two Gaussian densities positioned at the center of the trap. The ground-state energy in this case is found to be slightly higher than the off-center iteration in Fig. 6. The energies are here $E_0^{(1)}=3.779$ and $E_0^{(2)}=3.607$.

V. CONCLUSIONS

In this paper we have presented density calculations of a two-component condensate as a function of temperature. We have found symmetry breaking in the two-dimensional case, where the two-component condensates sitting at the center of the trap on top of each other possess a higher energy than the situation where the two condensates have separated and form two individual peaks. This is a case of spontaneous symmetry breaking. We also present a phase diagram that describes the different regions with a two-component condensate, one single condensate, and finally no condensate as a function of temperature and the interaction strength between the two different atoms. The phase diagram has been presented for three different pairs of particle numbers and calculated in three dimensions with spherical symmetric external potentials. This means that we cannot see the symmetry breaking that we saw in the two-dimensional calculations, which in fact gave an asymmetric solution in the symmetrical situation. The Hartree-Fock equations do not describe the transition region well because they neglect all critical fluctuations. They do, however, give us an idea of what may be happening around the transition point. At some critical particle number we find a region where it is possible, by changing the temperature at fixed interaction strength w, to go from a two-component condensate to two noncondensed gases.

In these calculations, we have only used a few hundred particles. Increasing the number of particles to realistic values ($\sim 10^6$) is beyond the capacity of available computers. So is a full treatment of totally asymmetric three-dimensional traps. With this small number of particles, the interaction strength w needs to be chosen unrealistically large to bring out the observed features. The small number of particles may give rise to finite-size effects as, for instance, regions with an inconsistent fraction of condensate particles calculated from the two-component condensate equations and the single-condensate equations. With increasing particle number, we may expect the inconsistency to disappear and give a crossing from a two-component condensate into a phase with two normal components for all interaction strengths w.

The numerics was performed with a grid method in the three-dimensional spherically symmetric case. This is a very stable and fast method. The only drawback is that it can in practice only be used in situations where the problem is effectively reduced to a one-dimensional one. The expansion

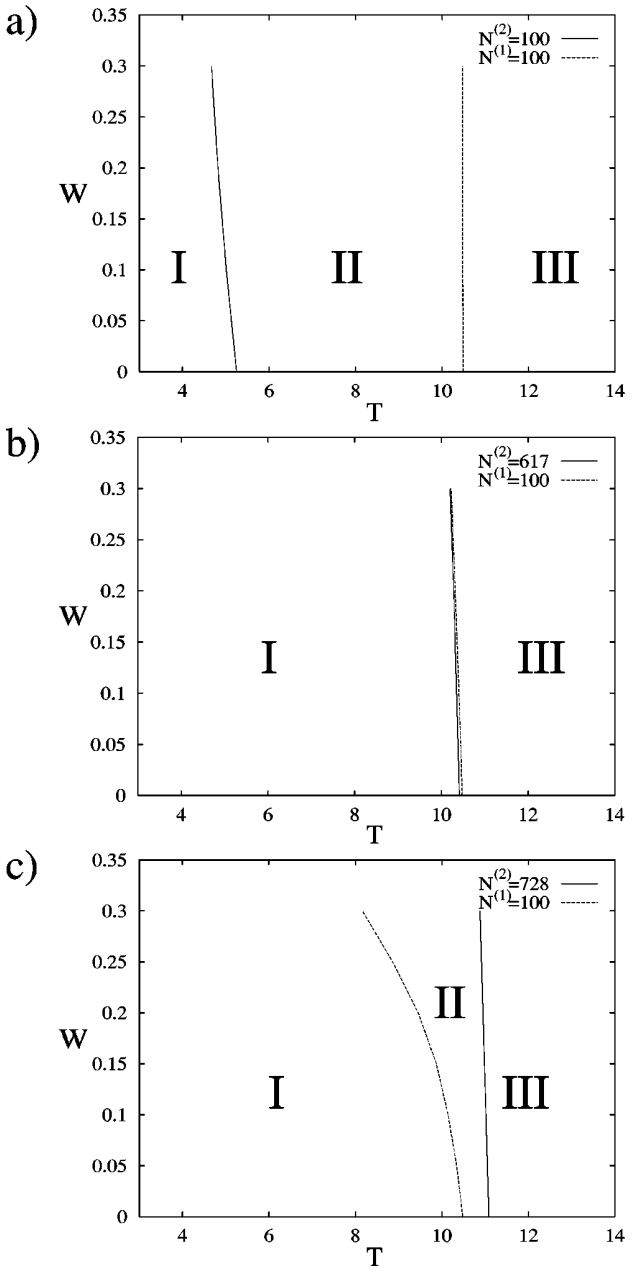

FIG. 8. Phase diagram described for three different pairs of particle numbers. In (a) we have $N^{(1)}=100$ and $N^{(2)}=100$. Here we can see that the transition line between regions II and III (one condensate and no condensate) is not sensitive to changes in w. In region II the $N^{(1)}$ particles are condensed and the $N^{(2)}$ particles are in the normal phase. In (b) we have $N^{(1)}=100$ and $N^{(2)}=617$ and we find a region where we have a transition between a two-component condensate (I) and no condensate (III). In (c) we have increased the relative particle number to $N^{(1)}=100$ and $N^{(2)}=728$. Region I with the two-component condensate is strongly suppressed as a function of w, whereas the transition between one condensate and no condensate (II and III) is not sensitive to changes in w. In this case, for region II, the $N^{(2)}$ particles are condensed and the $N^{(1)}$ particles are in the normal phase.

method, on the other hand, is very fragile in the two-dimensional calculations and great care has to be taken in order not to get runaway iterations that do not converge to physically stable solutions.

What about the possibility of observing the symmetry breaking in the laboratory? We notice that such an experiment poses tremendous technical difficulties. The sample has to be situated in a perfectly symmetric environment in order to avoid all technically induced asymmetries. The interaction potentials v_1 and v_2 we have used are of realistic orders of magnitude (in our scaled units); the mutual interaction w is expected to be of similar strength. In order to display the symmetry-breaking effects clearly, we have increased the mutual interaction up to 30 times its realistic value; otherwise the effects are minute and unobservable. No doubt the symmetry breaking occurs then too, but both the energy differences and the separations are so small that no conceivable method is likely to observe them. However, the influence on condensate 1 by condensate 2 is given by terms of the form $wN_{\alpha_0}^{(2)}|\phi_{\alpha_0}|^2$ (and vice versa); see Eqs. (29)–(32). This shows that if the traps could be designed such that condensate 2, say, would greatly exceed condensate 1 in density, then this could compensate for a weaker w; the reverse effect would then be negligible. Condensate 2 would remain as if condensate 1 did not exist, but its presence would push condensate 2 out from the center of the trap, thus affecting the symmetry breaking. How big a difference is needed depends on the sensitivity of the method of observation. In the real experiments, however, the atomic parameters determine the ratio between the condensates and some novel experimental technique is needed if this is to be varied.

Finally, we speculate on some features observed in our numerical computations. They may be due only to shortcomings of the numerical approach or limitations of the HF method, but they point to interesting possibilities in the behavior of the real systems.

First we look at situations like in Fig. 8(b). There the two-condensate and no-condensate boundaries are very close to each other; they may in fact be found to cross. In such regions, we find that the critical temperatures found from the two-condensate and from the single-condensate sides are inconsistent. If we could trust the HF calculations, this may indicate a hysteresis signaling a change to a first-order transition for one of the components. No such conclusion can be proven from the HF approach, but it points to the possibility that the change of one component can qualitatively affect the behavior of the other one even to the extent that its order may change.

Second, the use of too few states in the calculations gives a distorted and asymmetric solution. In two dimensions and for not too high temperatures ($\beta=1.0$), we get smooth densities for about ten states in each direction. Because of the unrealistically large values for w used, the two condensates repel each other strongly. This shows up as a drift instability, which eventually develops into an oscillational instability in the solution if the computer iteration is continued well after a stable solution is found. It seems that this can be overcome by increasing the number of states involved. The physical contents of our numerical observation may be that it signals the breakup of a solution only locally stable. Thus we find it to occur much more readily for the symmetric situation, whereas the asymmetric solutions are much more stable.

We have thus found our numerics to indicate the change of order of the transition and the instability of some locally stable solutions owing to the interaction between the two

condensates. Admittedly neither our numerical method nor our theoretical formulation (HF) allows any claims to the reality of the effects. They do, however, offer challenging possibilities for further experimental and theoretical investigations.

Unfortunately, it seems to be difficult to approach these problems from the two-component Gross-Pitaevskii equations. As these omit the atoms above the condensate, it is difficult to compute the effects on one condensate by the properties of the other one. On the other hand, any phase transition theory superior to the HF approach appears to offer unsurmountable computational difficulties. What progress can be achieved on these difficult questions remains to be seen.

[1] M. H. Anderson, J. R. Ensher, M. R. Matthews, C. E. Wieman, and E. A. Cornell, Science **269**, 198 (1995).
[2] C. C. Bradley, C. A. Sackett, J. J. Tollett, and R. G. Hulet, Phys. Rev. Lett. **75**, 1687 (1995).
[3] K. B. Davies, M.-O. Mewes, M. R. Andrews, N. J. van Druten, D. S. Durfee, D. M. Kurn, and W. Ketterle, Phys. Rev. Lett. **75**, 3969 (1995).
[4] D. S. Jin, J. R. Ensher, M. R. Matthews, C. E. Wieman, and E. A. Cornell, Phys. Rev. Lett. **77**, 420 (1996).
[5] M.-O. Mewes, M. R. Andrews, N. J. van Druten, D. M. Kurn, D. S. Durfee, and W. Ketterle, Phys. Rev. Lett. **77**, 416 (1996).
[6] M. R. Andrews, M.-O. Mewes, N. J. van Druten, D. S. Durfee, D. M. Kurn, and W. Ketterle, Science **273**, 84 (1996).
[7] M.-O. Mewes, M. R. Andrews, N. J. van Druten, D. M. Kurn, D. S. Durfee, C. G. Townsend, and W. Ketterle, Phys. Rev. Lett. **77**, 988 (1996).
[8] C. J. Myatt, E. A. Burt, R. W. Ghrist, E. A. Cornell, and C. E. Wieman, Phys. Rev. Lett. **78**, 586 (1997).
[9] C. C. Bradley, C. A. Sackett, and R. G. Hulet, Phys. Rev. Lett. **78**, 985 (1997).
[10] M. Edwards and K. Burnett, Phys. Rev. A **51**, 1382 (1995).
[11] D. A. W. Hutchinson, E. Zaremba, and A. Griffin, Phys. Rev. Lett. **78**, 1842 (1997).
[12] B. D. Esry, C. H. Greene, J. P. Burke, and J. L. Bohn, Phys. Rev. Lett. **78**, 3594 (1997).
[13] P. Öhberg and S. Stenholm, J. Phys. B **30**, 2749 (1997).
[14] D. A. Huse and E. D. Siggia, J. Low Temp. Phys. **46**, 137 (1982).
[15] V. V. Goldman, I. F. Silvera, and A. J. Leggett, Phys. Rev. B **24**, 2870 (1982).